Turkish Journal of Physics

Volume 38 | Number 2 Article 6

1-1-2014

Analogue and digital analysis of the effects of some parameters in determination of the best experimental energy resolution

ELİF EBRU ERMİŞ

GÖZDE TEKTAŞ

ERCAN PİLİÇER

CÜNEYT ÇELİKTAŞ

JIRI PECHOUSEK

Turkish Journal of Physics

http://journals.tubitak.gov.tr/physics/

Research Article

Turk J Phys
(2014) 38: 203 – 213

doi:10.3906/fiz-1401-10

Analogue and digital analysis of the effects of some parameters in determination of the best experimental energy resolution

Elif Ebru ERMİŞ[1,*], Gözde TEKTAŞ[1], Ercan PİLİÇER[2], Cüneyt ÇELİKTAŞ[1], Jiri PECHOUSEK[3]

[1]Department of Physics, Faculty of Science, Ege University, Bornova, İzmir, Turkey
[2]Department of Physics, Faculty of Arts and Science, Uludağ University, Görükle, Bursa, Turkey
[3]Department of Experimental Physics, Regional Centre of Advanced Technologies and Materials, Palacky University, Olomouc, Czech Republic

Received: 21.01.2014 • **Accepted:** 21.04.2014 • **Published Online:** 11.06.2014 • **Printed:** 10.07.2014

Abstract: The gamma-ray energy spectrum of ^{137}Cs was obtained according to different parameters such as preamplifier capacitance, the amplifier's coarse gain level, power supply voltage for the detector, and source-to-detector distance. This investigation was performed with both analogue and digital methods. In order to examine the effects of these parameters on energy resolution, a NaI(Tl) inorganic scintillation detector was used. In addition, the gamma energy spectrum of the radioisotope was obtained by means of FLUKA, which is one of the Monte Carlo simulation programmes. Energy resolution of the detector by these 3 methods was calculated. These resolution values were compared with each other. Effects of the parameters above on the resolutions from analogue and digital methods were discussed.

Key words: Analogue and digital data acquisition, NaI(Tl) inorganic scintillation detector, FLUKA MC simulation method

1. Introduction

For detectors that are designed to measure the energy of incident radiation, the most important factor is energy resolution. This is the extent to which the detector can distinguish 2 close-lying energies. In general, the resolution can be measured by sending a monoenergetic beam of radiation into the detector and observing the resulting spectrum. Ideally, of course, one would like to see a sharp delta-function peak. In reality, this is never the case and one observes a peak structure with a finite width, usually Gaussian in shape. This width arises because of fluctuations in the number of ionisations and excitations produced [1].

The energy resolution in percentage of a detector (R) is calculated with the following equation:

$$R = \frac{B - A}{E_\gamma} \times 100\%, \tag{1}$$

where E_γ is the channel number or energy corresponding to maximum peak count, and A and B are minimum and maximum channel numbers, respectively, corresponding to the full width at half maximum of a photopeak. These quantities can be seen in Figure 1. Note that A, B, and E_γ must all be in the same units (either keV or channel number on a multichannel analyser) [2].

*Correspondence: elermis@hotmail.com

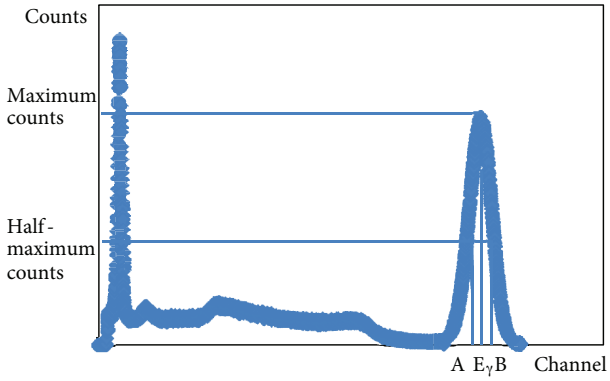

Figure 1. Used quantities in the calculation of energy resolution [2].

Most of the inorganic scintillators are crystals of the alkali metals, and in particular alkali iodides, that contain a small concentration of an impurity [3]. In addition to its efficient light yield, sodium iodide doped with thallium [NaI(Tl)] is almost linear in its energy response [4]. Of all the scintillators existing on the market, NaI(Tl) is the most widely used for the detection of γ-rays. NaI(Tl)'s relatively high density (3.67×10^3 kg/m^3) and high atomic number combined with the large volume make it a γ-ray detector with very high efficiency [3].

A new approach in the design of computer-based measurement systems can be seen in the use of up-to-date measurement, control, and testing systems based on reliable devices. Digital signal processing (DSP) is used in all engineering areas, such as in nuclear physics experiments, to replace conventional analogue systems and to build measurement and test systems with an easy configuration, user-friendly interface, and possibility to run sophisticated experiments. Nuclear DSP systems are commonly realised by the virtual instrumentation (VI) technique as performed in the LabVIEW graphical programming environment. The advantages of this approach lie in the use of ready-to-start measurement functions (DSP algorithms), in instrument drivers delivered with measurement devices, and in the possibility to improve a particular system when new algorithms, drivers, or devices are available [5].

The Monte Carlo (MC) method simulates the interactions of radiations with matter. MC simulation can be demonstrated as a black box to which we have to provide some input data, such as details of geometry of the radiation source, target and medium, type of radiation, energy, and direction of radiation flight. The black box diagram of a MC code is shown in Figure 2 [6].

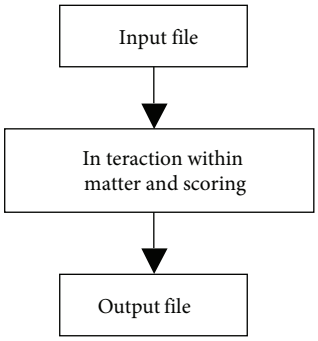

Figure 2. Black box of a MC code [6].

FLUKA is one of the MC programmes. The major reason for the design and development of FLUKA

MC is that the implementation and improvement of modern physical models are very important. Interaction and propagation of matter of any particles can be simulated by means of FLUKA [7,8].

Experimental energy spectra of ^{137}Cs were achieved by using different detector types in various studies [9–14]. MC simulation was used to determine gamma-ray response functions of a NaI(Tl) detector by Shi et al. [15]. The theoretical energy spectrum of ^{137}Cs was given by Ashrafi et al. via the Geant4 MC method [16]. The FLUKA MC method was also used to determine mass attenuation coefficients by Demir et al. [17]. Borio di Tigliole et al. calculated the response function of a neutron detector by means of FLUKA MC, as well [18]. Energy and time measurements were carried out using the VI technique by Pechousek et al. [19].

In this work, ^{137}Cs gamma energy spectra were obtained by analogue, digital, and theoretical methods with a multichannel analyser (MCA), a digitiser, and a MC programme. In addition, the effects of some parameters such as preamplifier capacitance, coarse gain settings of the main amplifier, detector bias level, and source-to-detector distance on the energy resolution of the used detector were investigated by analogue and digital data acquisition.

2. Experimental

A NaI(Tl) scintillation detector whose dimensions were 7.62 cm $\times$ 7.62 cm and a ^{137}Cs radioisotope as a point type gamma source were used in this study. The activity and half-life of the source are 5 μCi and 30.3 years, respectively [http://www.ezag.com/fileadmin/ezag/user-uploads/isotopes/pdf/EZIP_Ref__Cal_Catalog.pdf].

A block diagram of the used gamma spectrometer is shown in Figure 3.

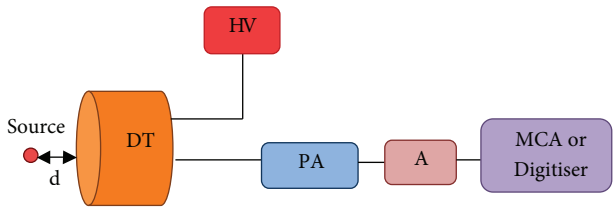

Figure 3. Block diagram of the used gamma spectrometer. HV: High-voltage supplier, DT: detector with photomultiplier tube, PA: preamplifier, A: main amplifier, MCA: multichannel analyser, d: source-to-detector distance.

In the setup in Figure 3, the detector output was sent to a preamplifier (PA, ORTEC 113), and its output was forwarded to a main amplifier (A, ORTEC 485). The amplifier output was connected to a MCA (ORTEC Trump 8K) to obtain the gamma energy spectrum of the source. The gamma energy spectrum of ^{137}Cs was also obtained by means of the digitiser. For this process, the MCA was substituted with a digitiser (NI 5133), as can be seen in Figure 3.

The output signal shape of the main amplifier is shown in Figure 4. A bipolar signal was used in the experiments to get rid of baseline shift.

The preamplifier capacitances were first changed to the values given in Table 1, and the energy spectra for each capacitance were acquired. The energy resolution values of the detector were calculated for each preamplifier capacitance value. Second, energy spectra and energy resolution values were obtained by changing the coarse gain settings of the main amplifier to 2, 4, and 8. Third, the effect of the detector bias level on the energy resolution values was investigated. For this purpose, the detector bias level was set to 800, 900, and 1000 V, respectively, and the energy resolution values for these bias levels were calculated. Finally, energy resolution values were determined by changing the source-to-detector distance according to the amounts given in Table 1.

These processes were carried out by using both the MCA and the digitiser. The graphs of the energy resolution values versus preamplifier capacitance, amplifier's coarse gain, power supply voltage, and source-to-detector distance were plotted for analogue and digital methods.

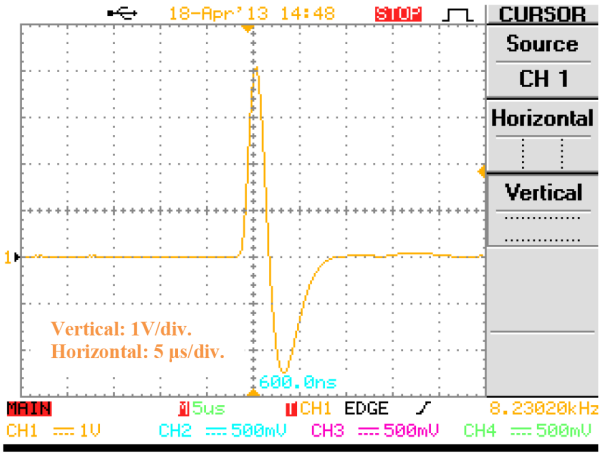

Figure 4. The output signal shape of the main amplifier.

Table 1. Preamplifier capacitance, main amplifier's coarse gain, power supply voltage, and source-to-detector distance values.

PA capacitance (pF)	100
	200
	500
	1000
Amplifier's coarse gain level	2
	4
	8
Power supply voltage (V)	800
	900
	1000
Source-to-detector distance (cm)	2
	4
	6
	8
	9.5

DSP systems use a device that digitises an analogue signal. A digitiser records the output signal from the radiation detector as an unprocessed signal or can acquire pulses coming through the signal amplifier or another preprocessing module. In the acquired signal, the pulse represents the nuclear event registration, and the amplitude of the peaks generally depends on the detected energy [5]. A LabVIEW programme that is run with a DSP system was used to achieve the digital energy spectrum of the used radioactive source in this work.

The theoretical energy spectrum of ^{137}Cs was obtained to compare it to the experimental spectrum. For this purpose, the FLUKA MC simulation programme was used. FLUKA (ver. 2011.2b) was installed on an Ubuntu (ver. 11.04) operating system. A view of the source and detector construction in the programme can be seen in Figure 5.

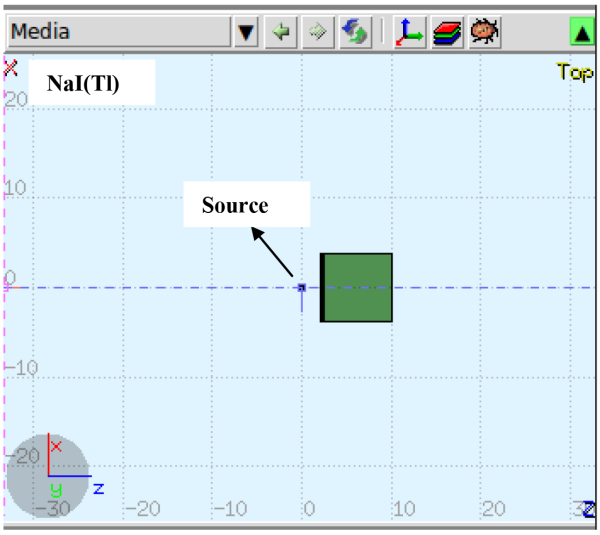

Figure 5. Position of the detector and the source in FLUKA.

3. Results

Preamplifier capacitance settings were changed and the obtained results are shown in Table 2.

Table 2. Photopeak counts, resolution, and the amplitude of the main amplifier output values with respect to the different preamplifier capacitance settings for analogue and digital methods.

Preamplifier capacitance (pF)	Photopeak counts (analogue)	Photopeak counts (digital)	Energy resolution (analogue) (%)	Energy resolution (digital) (%)	Amplitude of the main amplifier output (V)
100	5215 ± 55	7119 ± 53	6.56 ± 0.01	5.20 ± 0.26	4.12
200	8131 ± 30	8354 ± 23	6.86 ± 0.15	5.86 ± 0.32	2.56
500	17,455 ± 65	21,203 ± 64	6.72 ± 0.25	4.79 ± 0.03	1.28
1,000	32,526 ± 124	50,898 ± 93	6.10 ± 0.06	4.38 ± 0.30	0.62

Although the best energy resolution was obtained at the capacitance of 1000 pF, this value was not set as the optimum capacitance value because the energy spectrum shrank to the lower-energy region at this capacitance. Since a number of counts accumulated in one channel instead of a few channels, photopeak counts were raised at higher preamplifier capacitances (Table 2). In this part of the study, the applied power supply voltage to the detector was stabilised so that the number of electrons in the photomultiplier tube remained constant. Because the amplitude of the main amplifier output was inversely proportional to increasing preamplifier capacitance, the optimum capacitance value was set as 100 pF. In addition, obtained photopeak counts and energy resolution values, which were acquired by analogue and digital methods, were in accordance with each other (Table 2; Figure 6).

Amplifier coarse gain was set to 2, 4, and 8 factors, respectively, for the comparison of the resolution results. The obtained photopeak counts, resolution, and amplitude of the main amplifier output values are shown in Table 3 and Figure 7.

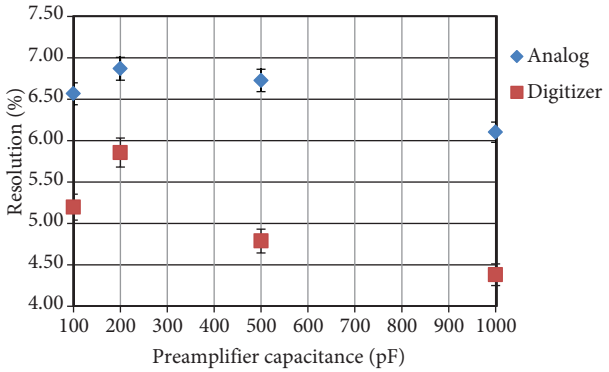

Figure 6. Energy resolution vs. preamplifier capacitance for analogue and digital methods.

Table 3. Photopeak counts, resolution, and the amplitude of the main amplifier output values corresponding to the different amplifier coarse gain settings for analogue and digital methods.

Amplifier coarse gain	Photopeak counts (analogue)	Photopeak counts (digital)	Energy resolution (analogue) (%)	Energy resolution (digital) (%)	Amplitude of the main amplifier output (V)
2	19,785 ± 41	22,758 ± 98	6.42 ± 0.00	4.60 ± 0.17	1.06
4	9866 ± 23	15,280 ± 70	6.84 ± 0.01	4.98 ± 0.09	2.20
8	5339 ± 30	7119 ± 53	6.92 ± 0.02	5.20 ± 0.26	3.92

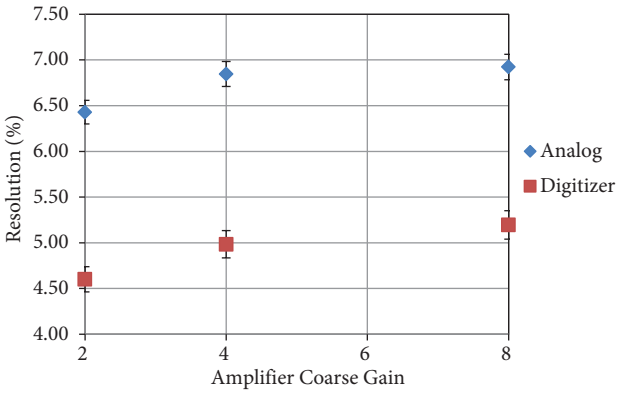

Figure 7. Energy resolution vs. amplifier's coarse gain for analogue and digital methods.

When the amplifier coarse gain was set to 2 and 4, the energy spectra shrank and accumulated in the lower-energy region. In addition, photopeak counts decreased as the amplifier coarse gain increased since the dead time of the system enlarged. Although the amplitude of the main amplifier's output was normally proportional to increasing coarse gain value, the data could not be acquired at higher than the coarse gain level of 8 because of the spectrum broadening to outside of the MCA screen. Thus, the optimum amplifier coarse gain was fixed as 8. These expressions were valid for both the analogue and digital methods.

Various power supply voltages were applied to the detector according to the values in Table 1, and the obtained photopeak counts, resolution, and amplitudes of the main amplifier output were determined (Table 4; Figure 8).

Table 4. Photopeak counts, resolution, and the amplitude of the main amplifier output values with respect to the different power supply voltage settings for analogue and digital methods.

Power supply Voltage (V)	Photopeak (analogue) counts	Photopeak counts (digital)	Energy resolution (analogue) (%)	Energy resolution (digital) (%)	Amplitude of the main amplifier output (V)
800	25,075 ± 89	41,167 ± 88	6.75 ± 0.14	4.57 ± 0.23	0.84
900	10,586 ± 28	11,925 ± 92	6.93 ± 0.00	5.02 ± 0.25	1.84
1,000	4885 ± 33	7119 ± 53	7.16 ± 0.08	5.20 ± 0.26	4.72

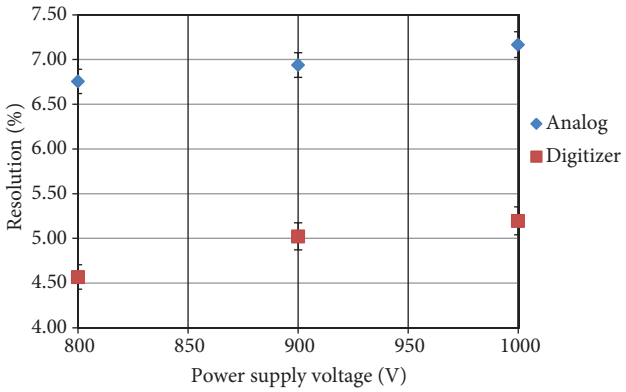

Figure 8. Energy resolution vs. power supply voltage for analogue and digital methods.

As can be seen in Table 4, the amplitude of the main amplifier output increased with the increasing power supply voltage under the constant preamplifier capacitance (100 pF) for both methods. Moreover, the photopeak counts decreased towards the higher power supply voltages due to the dead time of the system, and the energy resolution deteriorated since peak broadening occurred. Under these circumstances, the optimum power supply voltage for the detector was determined as 1000 V.

Finally, source to detector distance was changed to the values given in Table 1 and the obtained results are shown in Table 5. The best resolution was obtained at the source-detector distance of 4 cm for both methods (Table 5; Figure 9).

Table 5. Photopeak counts, resolution, and the amplitude of the main amplifier output values with respect to the different source-to-detector distances for analogue and digital methods.

d (cm)	Photopeak counts (analogue)	Photopeak counts (digital)	Energy resolution (analogue) (%)	Energy resolution (digital) (%)	Amplitude of the main amplifier output (V)
2	8314 ± 31	10,660 ± 42	6.83 ± 0.02	5.71 ± 0.09	4.48
4	4752 ± 42	7119 ± 43	6.63 ± 0.01	5.20 ± 0.26	4.56
6	3054 ± 32	4614 ± 19	6.73 ± 0.06	5.45 ± 0.19	4.00
8	2210 ± 29	3229 ± 23	6.90 ± 0.12	6.22 ± 0.18	3.84
9.5	1710 ± 25	2636 ± 8	6.83 ± 0.08	6.23 ± 0.20	4.08

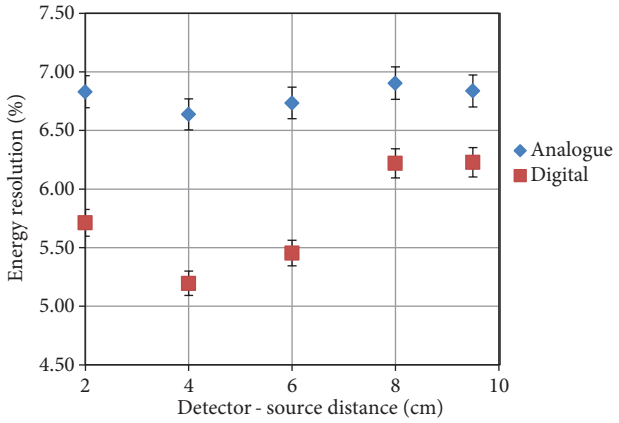

Figure 9. Energy resolution vs. source-to-detector distance for analogue and digital methods.

In Tables 2–5, each measurement, except for the amplitudes of the main amplifier output, was repeated 3 times, and the averages together with the standard deviations of the results were calculated. Standard deviations were added to the averages.

For the best energy resolution, optimum coarse gain level of the main amplifier, detector bias level, and source-to-detector distance were also determined. Gamma energy spectra of the used radioisotopes were acquired via these parameters for both methods (Figures 10a and 10b). Experimental photopeak energy resolution values with optimum parameters for the analogue and digital methods were calculated as 6.56% (Figure 10a) and 5.20% (Figure 10b), respectively. The horizontal and vertical axes in Figure 10 correspond to the channel numbers and counts, respectively.

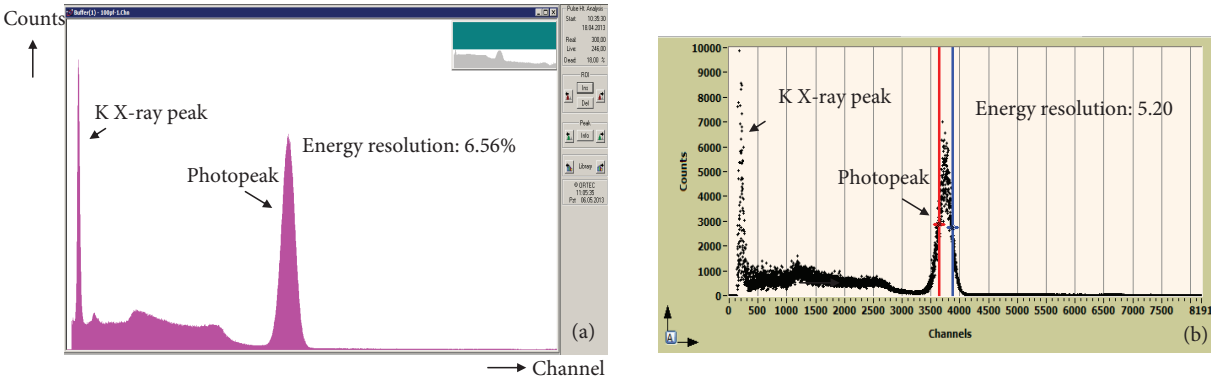

Figure 10. Gamma energy spectrum of ^{137}Cs from (a) MCA (analogue) and (b) digitiser (digital).

In Figure 11, the obtained theoretical gamma energy spectrum via the FLUKA MC programme is shown for comparison. The photopeak energy resolution value was calculated as 6.77% from this spectrum (Figure 11).The spectra from the MCA, the digitiser, and the FLUKA programme were given in separate figures because the software programmes were not compatible with each other.

4. Discussion and conclusion

Gamma energy spectra of a ^{137}Cs radioisotope were obtained through different methods: analogue, digital, and theoretical. The spectrometer in Figure 3 consisted of a NaI(Tl) scintillation detector that was used for

both analogue and digital methods to obtain experimental energy spectra. The theoretical energy spectrum was acquired by means of the FLUKA MC programme. In Section 2, the effect of preamplifier capacitance, coarse gain setting of the main amplifier, detector bias level, and source-to-detector distance on the energy resolution of the detector were investigated for analogue and digital methods.

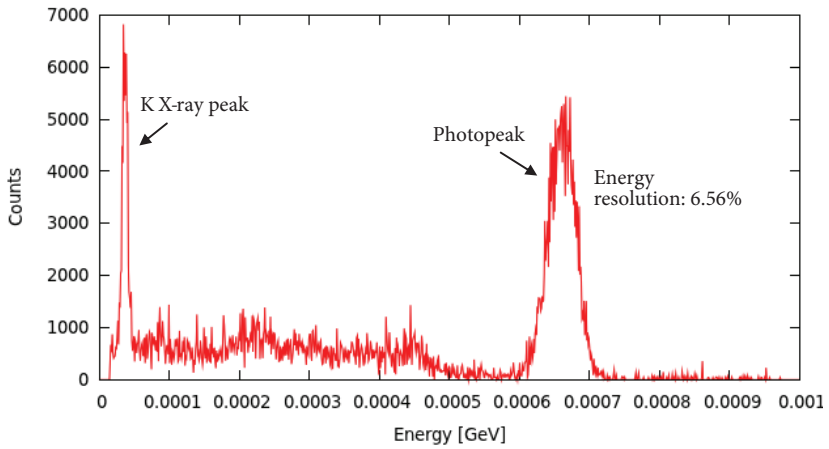

Figure 11. Theoretical gamma energy spectrum from the FLUKA programme (GeV is the standard energy unit).

Energy resolution variation according to various preamplifier capacitances was investigated for both experimental methods (Table 2; Figure 6). Since the energy spectrum shrank to the lower-energy region at higher preamplifier capacitance, lower capacitance values were suggested by the obtained results for the best energy resolution. It was found that the obtained results from the analogue and digital methods were in accordance with each other, as can be seen from Table 2 and Figure 6.

It was observed that the energy resolution of the detector deteriorated as the coarse gain level of the main amplifier was increased in both methods (Table 3; Figure 7). In addition, the photopeak counts were decreased due to the dead-time increment and the peak broadening. When the coarse gain level of the main amplifier was increased, the spectrum shifted to upper channel numbers. For this reason, its coarse gain could not be set higher than the eighth multiplication level.

As the bias level of the detector was increased, a decline in photopeak counts and a rise in the amplitude of the main amplifier output were noticed. Photopeak counts were diminished since the dead time of the system was raised with the rising power supply voltages (Table 4; Figure 8). The power supply voltages of less than 800 V could not be applied to the detector because the energy spectrum was not acquired below this voltage. However, detector bias levels greater than 1000 V could not be set, since the energy spectrum was outside of the maximum MCA channel range (8k). These situations were valid for both the analogue and digital methods (Table 4; Figure 8).

Increasing the source-to-detector distance naturally led to the degradation of the photopeak counts because of energy loss and scattering of the photons (Table 5; Figure 9). The best analogue and digital energy resolution values were obtained at the source-to-detector distance of 4 cm, as can be seen in Table 5 and Figure 9. Energy resolution values were deteriorated at the source-to-detector distance of 2 cm due to backscattering from the source surface.

For the best energy resolution, optimum preamplifier capacitance, amplifier coarse gain, power supply voltage for the detector, and source-to-detector distance were determined. The energy spectra of the radioisotope

from the analogue and digital experimental methods were obtained by using these optimum parameters (Figures 10a and 10b). Analogue and digital energy resolution values from Figures 10a and 10b were calculated as 6.56% and 5.20%, respectively.

The energy spectrum was also acquired with the FLUKA MC programme and the theoretical energy resolution was found to be 6.77% (Figure 11). Ashrafi et al. obtained the ^{137}Cs gamma energy spectrum by means of the GEANT4 MC method [16]. When a comparison was made between their theoretical spectrum and the one in this work, it was seen that the K X-ray peak was available in the presented spectrum via FLUKA MC method.

The digital energy resolution values were smaller than the analogue and theoretical ones. This means that the digital system has advantages for distinguishing very close peaks. In addition, the success of the digital method arises from its high sampling rate. Furthermore, distortion or noise, which are always present in any circuit, will easily alter the information in an analogue signal but will be less effective for a logic signal [1]. Consequently, the digital system is more preferable than the analogue one from the point of view of energy resolution.

Consequently, the optimum preamplifier capacitance, amplifier coarse gain, power supply voltage, and source-to-detector distance were determined to obtain the best energy resolution in this study. Furthermore, analogue and digital energy spectra were compared with the theoretical energy spectrum acquired by the FLUKA MC programme, and the harmony among all spectra was noticed. Ift was emphasised via this comparison that the optimum parameters for the spectrometer to be used should be first determined for the best results and experimental success. Additionally, it was concluded that the compatibility between the experimental and the theoretical results would be able to improve the optimum parameters for the spectrometers to be used.

Acknowledgements

This work was supported by the Scientific and Technological Research Council of Turkey (TÜBİTAK) under Project Nos. 197T087 and 111T571, and by the Centre of Science and Technology of Ege University (EBİLTEM) under Project No. 99 BIL 001. The authors acknowledge the support of the Operational Programme 'Research and Development for Innovations' of the European Regional Development Fund (CZ.1.05/2.1.00/03.0058), the Operational Programme 'Education for Competitiveness' of the European Social Fund (CZ.1.07/2.3.00/20.0155), and the Ministry of Education, Youth, and Sports of the Czech Republic.

References

[1] Leo, W. R. *Techniques for Nuclear and Particle Physics Experiments*; Springer: Berlin, Germany, 1987.

[2] Prekeges, J. *Nuclear Medicine Instrumentation*; Jones & Bartlett Publishers: Sudbury, MA, USA, 2011.

[3] Tsoulfanidis, N. *Measurements and Detection Radiation*; Taylor & Francis: London, UK, 1995.

[4] Turner, J. E. *Atoms, Radiation and Radiation Protection*; Wiley-VCH Verlag: Weinheim, Germany, 2007.

[5] Folea, S. In *Application of Virtual Instrumentation in Nuclear Physics Experiments*; Pechousek, J., Ed. InTech: Rijeka, Croatia, 2011, pp. 57–80.

[6] De Lima, J. J. P. *Nuclear Medicine Physics*; Taylor & Francis: London, UK, 2011.

[7] Ferrari, A.; Sala, P. R.; Fasso, A.; Ranft, J. *FLUKA: A Multi-Particle Transport Code INFN/TC-05/11, SLAC-R-773*; CERN: Geneva, Switzerland: 2005.

[8] Battistoni, G.; Cerutti, F.; Fasso, A.; Ferrari, A.; Muraro, S.; Ranft, J.; Roesler, S.; Sala, P. R. In *AIP Conference Proceedings: Proceedings of the Hadronic Shower Simulation Workshop 2006*; Albrow, M., Raja, R., Eds.; 2007, p. 31.

[9] Moszynski, M. *Nucl. Instrum. Meth. A* **2003**, *505*, 101–110.

[10] Wang, Y. J.; Patt, B. E.; Iwanczyk, J. S. *IEEE Trans. Nucl. Sci.* **1995**, *42*, 601–605.

[11] Nestor, O. H.; Huang, C. Y. *IEEE Trans. Nucl. Sci.* **1975**, *22*, 68–71.

[12] Kapusta, M.; Balcerzyk, M.; Moszynski, M.; Pawelke, J. *Nucl. Instrum. Meth. A* **1999**, *421*, 610–613.

[13] Shah, K. S.; Glodo, J.; Klugerman, M.; Higgins, W. M.; Gupta, T.; Wong, P. *IEEE Trans. Nucl. Sci.* **2004**, *51*, 2395–2399.

[14] Çeliktaş, C.; Ermiş, E. E.; Bayburt, M. *J. Radioanal. Nucl. Chem.* **2012**, *293*, 377–382.

[15] Shi, H. X.; Chen, B. X.; Li, T. Z.; Yun, D. *Appl. Radiat. Isot.* **2002**, *57*, 517–524.

[16] Ashrafi, A.; Anvarian, S.; Sobhanian, S. *J. Radioanal. Nucl. Chem.* **2006**, *269*, 95–98.

[17] Demir, N.; Tarım, U. A.; Popovici, M. A.; Demirci, Z. N.; Gürler, O.; Akkurt, I. *J. Radioanal. Nucl. Chem.* **2013**, *298*, 1303–1307.

[18] Borio di Tigliole, A.; Cesana, A.; Dolfini, R.; Ferrari, A.; Raselli, G. L.; Sala, P.; Terrani, M. *Nucl. Instrum. Meth. A* **2001**, *469*, 347–353.

[19] Pechousek, J.; Prochazka, R.; Prochazka, V.; Frydrych, J. *Nucl. Instrum. Meth.* **2011**, *637*, 200–205.